

- 40 57. Piqueux, S., Byrne, S., Kieffer, H. H., Titus, T. N., Hansen, C. J. Enumeration of
41 Mars years and seasons since the beginning of telescopic exploration. *Icarus*, **251**,
42 332-338 (2015).
- 43 58. Dickson, J. L., Head, J. W., Kulowski, M. Active flows at the Mars Science
44 Laboratory landing site: Results from a survey of Mastcam imagery through Sol 971.
45 Lunar Planet. Sci. Conf. 47, abstract #1726 (2016).
- 46 59. Dundas, C. M., McEwen, A. S. Slope activity in Gale crater, Mars. *Icarus*, **254**, 213-
47 218 (2015).
- 48 60. Sullivan, R., Thomas, P., Veverka, J., Malin, M., Edgett, K. S. Mass movement
49 streaks imaged by the Mars Orbiter Camera. *J. Geophys. Res.*, **106**, 23,607–23,633
50 (2001).
- 51 61. Baratoux, D., et al. The role of wind-transported dust in slope streaks activity:
52 Evidence from the HRSC data. *Icarus*, **183**, 30-45 (2006).
- 53 62. Chuang, F. C., Beyer, R. A., McEwen, A. S., Thomson, B. J. HiRISE observations of
54 slope streaks on Mars. *Geophys. Res. Lett.*, **34**, L20204, doi:10.1029/2007GL031111
55 (2007).
- 56

57 **Supplementary Table 1. Slope Measurement Locations**

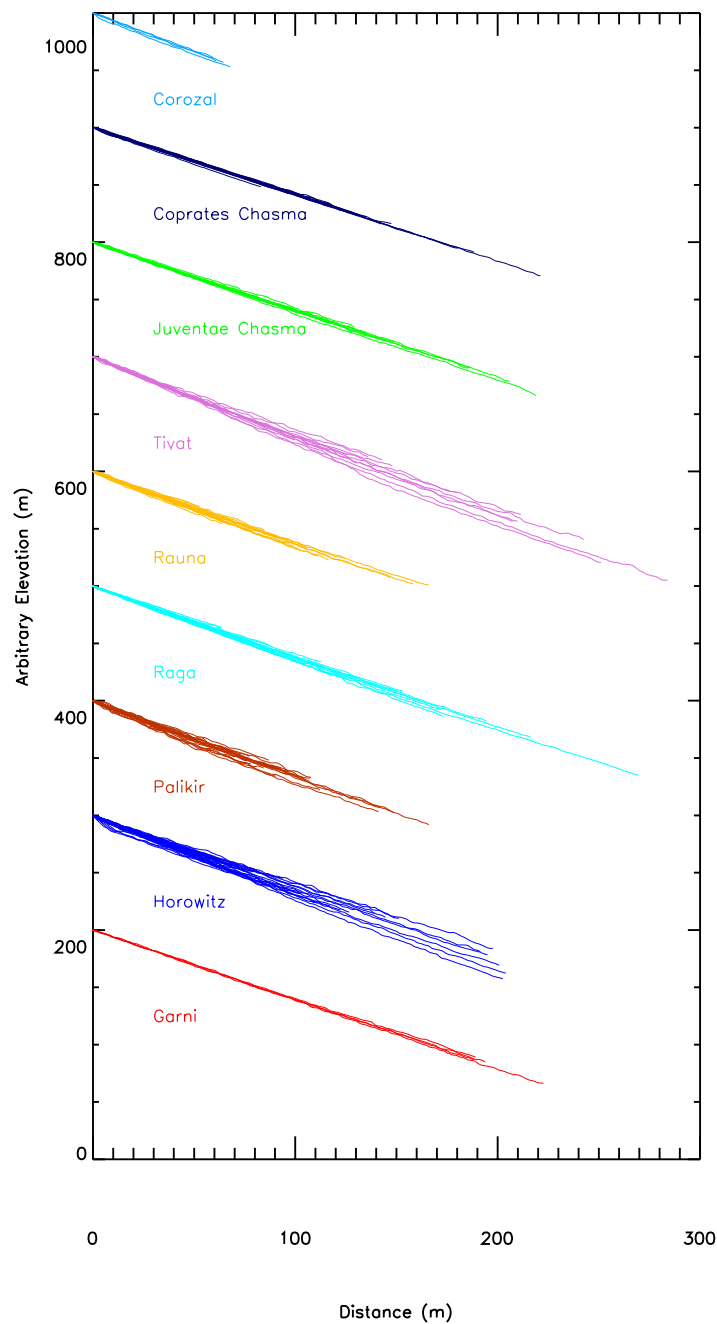
Location	Lat. ^a	Long. ^a	DTM ID and HiRISE Image	L _s	# Lineae
Rauna crater	35.3°	327.9°	DTEEC_034934_2155_034499_2155_A01 ESP_035923_2155	108°	15
Juventae Chasma	-4.7°	298.6°	DTEEC_030373_1755_030795_1755_A01 ESP_030373_1755	327°	9
Garni crater ^b	-11.5°	290.3°	DTEEC_027802_1685_028501_1685_A01 ESP_031059_1685	281°	4
Coprates Chasma	-13.1°	295.2°	DTEEC_034197_1670_033485_1670_A01 ESP_034197_1670	48°	17
Eos Chasma	-15.4°	309.5	DTEEC_039788_1645_039854_1645_A01 ESP_032667_1645	332°	22
Horowitz crater	-31.2°	140.8°	DTEEC_021689_1475_020832_1475_A01 PSP_005787_1475	334°	33
Corozal crater	-38.8°	159.5°	DTEEC_006261_1410_014093_1410_A01 PSP_006261_1410	354°	4
Palikir crater	-41.6°	202.1°	DTEEC_005943_1380_011428_1380_A01 PSP_005943_1380	341°	20
Tivat crater	-45.9°	9.5°	DTEEC_012991_1335_013624_1335_A01 ESP_023184_1335	324°	12
Raga crater	-48.1°	242.4°	DTEEC_014011_1315_014288_1315_A01 ESP_014011_1315	308°	15

58 ^aPlanetocentric latitude, east longitude.

59 ^bSouth-facing lineae.

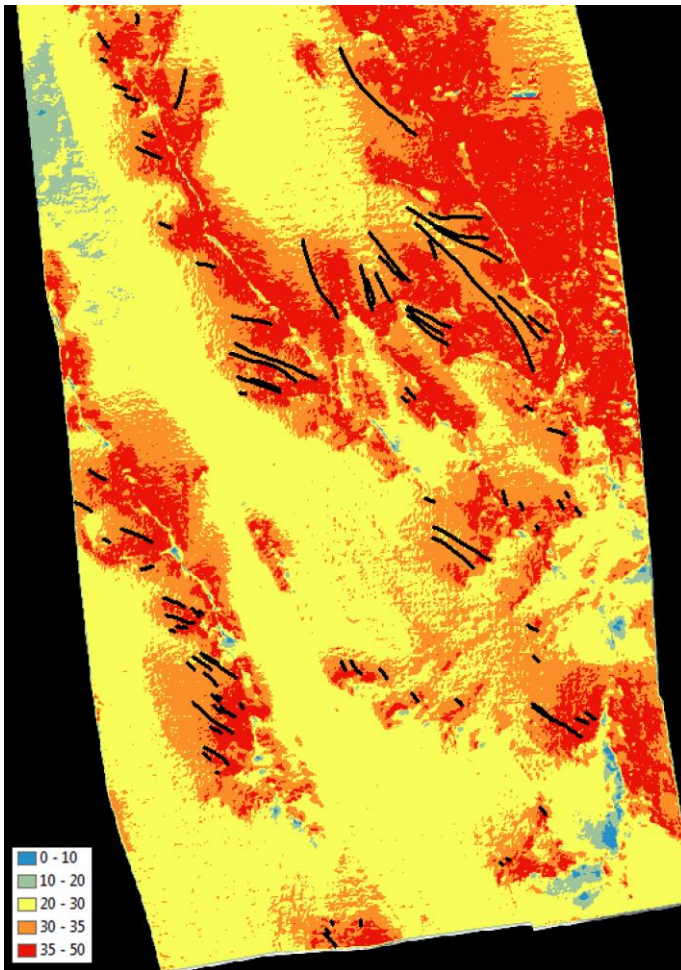
60

61



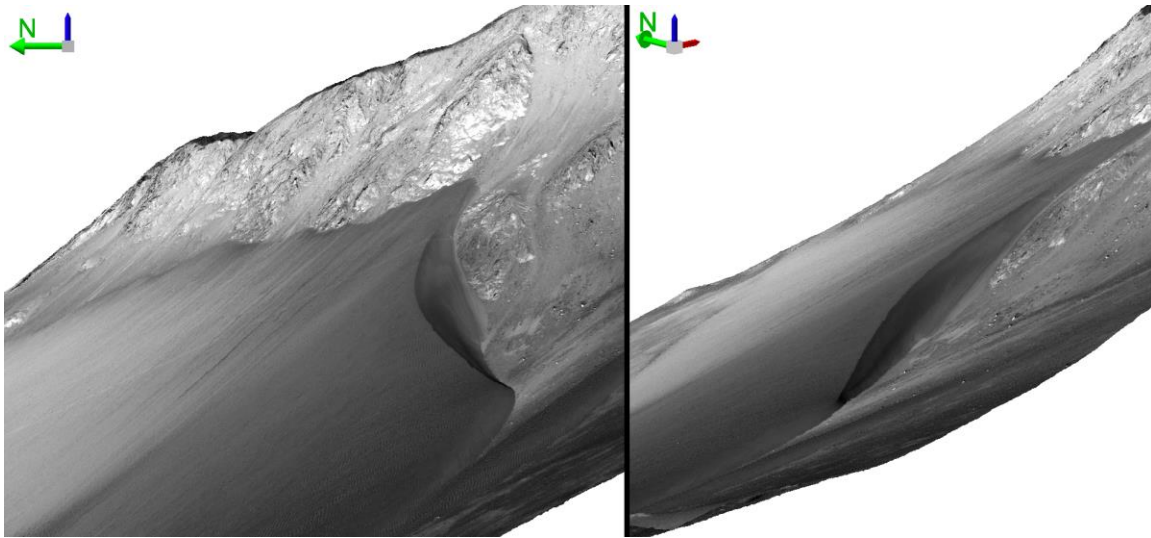
62
 63 **Supplementary Figure 1:** Slope profiles for RSL at nine of the ten locations examined.
 64 (Eos Chasma (Fig. S2) omitted due to greater range in length.) Elevations are arbitrarily
 65 offset to place the start of all the lineae from a particular location at a single reference
 66 elevation. Lineae range from straight to very slightly concave.

67

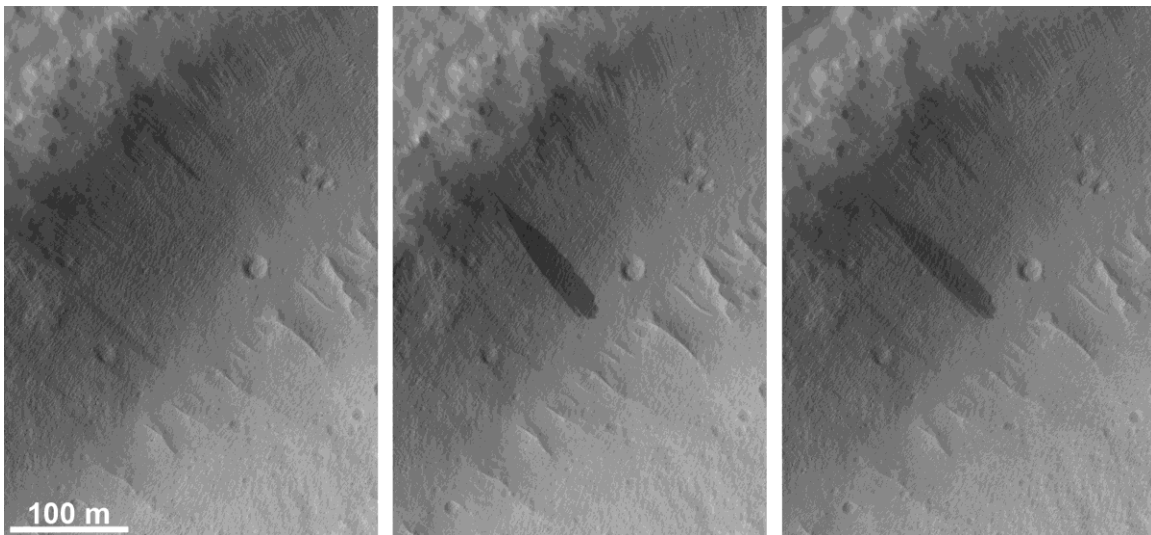


68
69
70
71
72
73
74
75
76
77
78
79
80

Supplementary Figure 2: Slope map of RSL site near Eos Chasma with selected lineae (from ESP_032667_1645) sketched in black. Lineae ranging from <30 m to >1.5 km long all terminate on slopes of 30–35°, the orange region of the map, mostly reaching to the yellow-orange boundary at 30°. Most such slopes have lineae, but some are not drawn because they are ill-defined and/or are difficult to distinguish from topography on east-facing slopes with stronger topographic shading. Long lineae (hundreds of meters in length) are found only where there is a long angle-of-repose slope available. (Slope map derived from a HiRISE DTM resampled to 10 m post spacing in order to reduce noise. Minor jitter effects are visible as a pattern of left-right trending bars, but are not large enough to affect interpretation of the slopes. The lineae in Table S1 are a subset of those in this figure with the highest-quality topography.)



81
 82 **Supplementary Figure 3:** Perspective views of the lineae and climbing dune shown in
 83 Fig. 2. Sand is advancing obliquely uphill and to the right. The left panel shows that
 84 lineae occur where sand advance is blocked by a steep outcrop, while a slipface occurs
 85 where the sand is not obstructed. The right panel shows that both the dark sandy surface
 86 below the slipface and the lighter material below the lineae are part of a smooth,
 87 continuous sediment body. Large ripples are present across the surface, indicating that the
 88 material is sandy. The stoss slope of this sand surface is unusually steep, at 30° , allowing
 89 reverse grainflows. Some RSL begin well upslope of the well-defined dune. (Perspective
 90 views generated by draping an orthorectified image over a DTM in Esri ArcScene®. Zero
 91 vertical exaggeration; blue vectors indicate vertical direction and green indicates north.
 92 HiRISE DTM DTEEC_046619_1665_045907_1665_A01.)
 93



94
 95 **Supplementary Figure 4:** Formation of a slope streak. These three HiRISE images show
 96 that the streak formed within a one-month interval and was subsequently unchanged over
 97 5.5 years. This is consistent with a single slope failure producing the flow, unlike RSL.
 98 (HiRISE images PSP_001364_2160 (Nov. 10, 2006), PSP_001760_2160 (Dec. 11,
 99 2006), and ESP_027776_2160 (June 29, 2012). North is up and light from the left in each

100 image. The slight appearance of rotation between panels is due to different viewing
101 geometry.)

102

103

104 **Caption for Supplementary Animation 1:** Grainflow activity on a sand dune slip face
105 (slope approximately 28°), resembling RSL. Lineae were present at $L_S=288^\circ$, along with
106 widespread dust devil tracks. They became more extensive through $L_S=338^\circ$, including
107 some incremental growth or overprinting. The lineae had faded by $L_S=50^\circ$ of the next
108 year, coincident with the disappearance of dust devil tracks. Changes continued on the
109 slipface through $L_S=124^\circ$, the low-pressure season when aeolian activity is reduced, but
110 did not produce distinct lineae because of a lack of surface dust. New lineae and many
111 dust devil tracks then formed sometime between $L_S=209 - 260^\circ$. (All image figures are
112 HiRISE cutouts from orthorectified images (credit: NASA/JPL/University of Arizona)
113 with north up and light from the left. The downhill direction on the slipface is towards the
114 bottom of the image.)

115

116 **Caption for Supplementary Animation 2:** Upslope ripple movement observed on an
117 RSL fan in Coprates Chasma. This demonstrates that in at least some locations sand-sized
118 grains can be resupplied by uphill movement. The ripples are of the same scale as the
119 large ripples observed by (47) and could be superposed by smaller bedforms. (Same
120 location shown in (11), but with extended time series.)

121

122

123